Proceedings of the International Conference on Industrial Engineering and Operations Management

Publisher: IEOM Society International, USA DOI: 10.46254/IN05.20250235
Published: November 6, 2025

Comparative Study and Performance Optimization of Local Beach Sands for Sustainable Abrasive Jet Machining of Mild Steel

Ajit Gaonkar
Mechanical Engineering Department,
Goa College of Engineering
(Affiliated to the Goa University)
Farmagudi, Ponda, Goa 403401, India
ajit@gec.ac.in

Rajesh S. Prabhu Gaonkar
Professor in Mechanical Engineering
Goa College of Engineering
(Affiliated to the Goa University)
Farmagudi, Ponda, Goa 403401, India
rpg@gec.ac.in

Abstract

Air Abrasive Jet Machining (AJM) is used to machine thin ductile and brittle sections, yet conventional abrasives (aluminium oxide, silicon carbide, and garnet) are mined resources with a significant environmental footprint. This study assesses sieved, washed beach sands from local Goan beaches as sustainable abrasives for AJM of 2 mm mild steel. The AJM rig was used, and five factors - air pressure (P), nozzle diameter (d_N), stand-off distance (S), abrasive flow rate (A), and impingement time (T) - were varied using a Taguchi L_{27} design. Material Removal Rate (MRR) and Kerf Taper Angle (KTA) were measured and optimized via the Mixed Aggregation by Comprehensive Normalization Technique (MACONT). d_N influenced MRR, whereas S dominated KTA. Benaulim sand (≈ #60) produced higher MRR but larger KTA, and Agonda sand (≈ #40), yielded lower MRR but smaller KTA. Optimal settings for Benaulim sand were 8 bar P, 2.5 mm d_N, 2 mm S, 470 g/min A and 600 s T, yielding MRR ≈ 0.00077 g/s and KTA ≈ 3.15° and for Agonda sand, 8 bar P, a 3 mm d_N, 2 mm S, 370 g/min A, and 540 s T, gave MRR ≈ 0.00043 g/s and KTA ≈ 0.28°. Compared with garnet (≈ #80) in Abrasive Water Jet Machining (AWJM), these beach sands have reduced MRR but delivered improved KTA, demonstrating their promise as low-cost, eco-friendly AJM abrasives.

Keywords

Taguchi Methodology, Material Removal Rate (MRR), Kerf Taper Angle (KTA), MACONT (Mixed Aggregation by Comprehensive Normalization Technique), Abrasive Jet Machining (AJM)

1. Introduction

Abrasive Jet Machining (AJM) and Abrasive Water Jet Machining (AWJM), which preserve mechanical properties and avoid thermal impacts, are excellent methods for the precise machining of complex composites and hard metals (Perec et al., 2021). AWJM operates at ultra-high pressures (about 6000 bar), enabling the cutting of materials up to 300 mm thick, whereas AJM utilizes a high-velocity air-abrasive stream, particularly useful for thin or sensitive substrates. Typical abrasive media such as silicon carbide, aluminium oxide and garnet are mined minerals, so their

extraction and disposal raise concerns about resource depletion and waste. In AWJM they make up roughly half of the process cost, prompting investigations into more economical and environmentally friendly alternatives (Karkalos et al., 2023). Recent studies have explored environmentally sustainable and recyclable abrasives, such as waste grinding wheel alumina, crushed glass, and organic substances like walnut shells; Palaniyappan et al. (2020). Karkalos et al. (2023) demonstrated that walnut shells can be utilized as an abrasive in AWJM; however, the Material Removal Rate (MRR) was much lower than that achieved with garnet as an abrasive. This study assesses locally produced beach sand as a sustainable abrasive in AJM for 2 mm mild steel, suggesting that little screening, washing, and drying might make this sand a cost-effective substitute for mined abrasives. Experiments were performed with a custom - built AJM test rig, featuring pressurized air, a tungsten carbide nozzle, and a dust extractor to reduce silica dust. Sands from Benaulim and Agonda beaches in Goa were statistically studied to investigate their performance differences in AJM. Air pressure (P), nozzle exit diameter (d_N), Stand-off Distance (S), abrasive flow rate (A), and impingement time (T), were the five control factors set in the Taguchi L_{27} orthogonal array Design of Experiment (DoE) to thoroughly evaluate the effects on response parameters. Tripathi et al. (2020) recognized MRR and KTA as critical indicators of cutting efficiency and precision. The experimental matrix consisted of 27 runs on 2 mm thick mild steel specimens to gather MRR and KTA data across the parameter space. The Mixed Aggregation by Comprehensive Normalisation Technique (MACONT) is an innovative multi-criteria decision-making (MCDM) method aimed at achieving a compromise solution that optimizes a high MRR while minimizing KTA, as demonstrated by Wen et al. (2020) and applied by Chatterjee et al. (2025). This research utilizes the same technique. The ideal control factor settings and responses derived from beach sand abrasives were compared with those from garnet to assess the enhancements. The results suggest a positive trend. With appropriate initial grading and conditioning of local beach sand, it could function as a sustainable, economical abrasive in AJM, providing improved cutting precision (lower KTA) relative to conventional garnet abrasives, despite reduction in MRR.

2. Literature Review

AJM is increasingly significant for producing precision features in both brittle and ductile materials, as it prevents thermal damage and is capable of machining a diverse array of materials, including glasses, ceramics, modern composites, and CFR-PLA variants; Hashish et al. (2024), Bayraktar et al. (2022), Kartal et al. (2025)). Although garnet, alumina and silicon carbide are effective cutting agents/ abrasives, mining them imposes significant environmental costs. Handling these materials also exposes operators to respirable crystalline silica, which carries health risks; Misra et al. (2023). Recent sustainability frameworks for machining emphasise minimising environmental impacts throughout the process chain; Elsheikh et al. (2024), Shokrani et al. (2024).

A significant deficiency is the insufficient examination of locally sourced, natural abrasives in AJM using comprehensive DoE methodologies. Motivated by recent AWJM research utilizing eco-friendly abrasives, such as walnut shell, which demonstrate viability despite some trade-offs; Karkalos et al. (2023), this study examines locally available beach sand as an economical, low-transport-emission abrasive with potential for circular usage in AJM i.e. Sustainable AJM.

Taguchi (DoE) is the established standard for rigorous factor screening and optimisation in AJM and AWJM. Common control factors encompass P, d_N, S, A, traverse speed, and T. Typical responses encompass MRR, KTA/ kerf taper width, and surface roughness. Several recent research in AJM/AWJM utilize an L_{27} orthogonal array for multi-factor, three-level designs, since it produces almost precise solutions with the least number of experimental runs; Anjaneyulu et al. (2023), BRN et al. (2024), Kannan et al. (2021).

MCDM is progressively employed to harmonize contradictory outcomes (e.g., optimizing MRR while reducing KTA). Recent AWJM articles employ TOPSIS, VIKOR, WASPAS, and their hybrids to rank parameter sets and identify compromise solutions with distinct trade-offs; Radomska-Żalas et al. (2023), Kawecka et al. (2024). Recent formulations, including MACONT within neutrosophic frameworks, have been studied for improving the AWJM process; Chatterjee et al. (2025). This study used MACONT MCDM to integrate Taguchi outcomes, producing weight-sensitive rankings that emphasize low KTA while reducing the trade-off on MRR.

Using beach sand gathered locally as an abrasive supports sustainability goals by reducing reliance on mined materials and cutting transport-related emissions. Taguchi–MCDM analyses indicate that such substitutes can still meet performance requirements. Current work on green machining highlights the need to choose alternative media and tune

process parameters to lessen environmental harm while maintaining quality; Shokrani et al. (2024), Karkalos et al. (2024).

3. Experimental Setup & Methodology

3.1 AJM Machine Setup

An Abrasive Jet Machine, as shown in Figure 1(a, b), designed and fabricated to conduct experimental runs using beach sand. The setup has three sections:

- The Abrasive Feed Section includes abrasive tank installed having a maximum storage capacity of 15 kg. The abrasive tank has integrated stirrer for consistent sand flow and a heater to maintains a temperature of 60°C to ensure moisture - free sand whose flow is regulated by a needle valve actuated by an electromagnet. This configuration allows the operator to select distinct sand flow rates for each Experimental run, facilitating proper control of the abrasive flow.
- Within the mixing and delivery section, a pipe links the abrasive hopper to the nozzle. An air-filtration and drying unit between them conditions the compressed air so that sand and air combine according to the settings chosen for each test.
- A 5 HP compressor fitted with a 120-litre receiver and delivering about 15 CFM provided the necessary air flow and pressure. A calibrated regulator enabled the pressure to be adjusted to suit different trial conditions.

Tungsten-carbide nozzles with exit diameters of 2 mm, 2.5 mm and 3 mm were used, all with a length of 25 mm. A manual adjustment permitted setting of the Stand-off Distance (S), and a digital timer controlled the jet's impingement duration on the workpiece. The workpiece is secured in the machining chamber with a clamp featuring a toughened glass door and an exhaust pipe for extracting dust produced during machining.

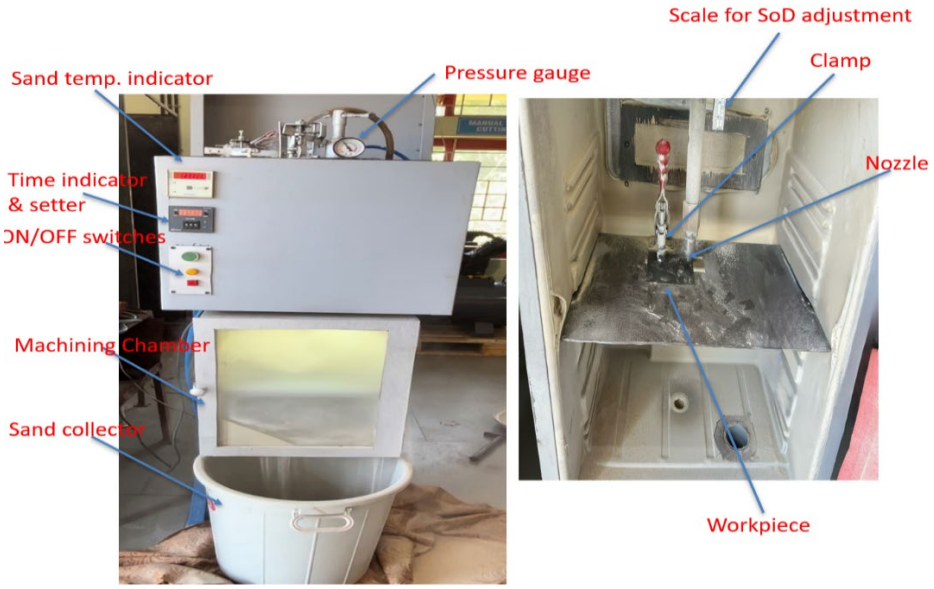

Figure 1. AJM experimental setup with (a) overall AJM machine
(b) inside view of machining chamber. (Chotilya et al.2020)

3.2 Abrasive Material and Workpiece

3.2.1 Beach sand as abrasive material

Sand intended for use as an abrasive was collected from the seashore at Benaulim Beach and Agonda Beach in South Goa. The suitability of the sand as an abrasive was evaluated in the laboratory using the procedures laid out in IS 1917:1991 and IS 1917:1992. Table 1 & Table 2 show its chemical composition, and Table 3 & Table 4 shows sand particle size distribution. The sand from Benaulim Beach is ideal for abrasive applications due to

its high silica concentration of 89.10% and minimal impurities. Particle-size analysis showed that over 84 % of the sample lay within the effective abrasive size range of 60–100 mesh. This distribution implies that the material could function as a reliable, more sustainable abrasive for abrasive-jet machining. Similarly, Agonda Beach sand is ideal for abrasive applications due to its high silica concentration of 85.23% and minimal impurities. Over 70% of the sample is categorized within the effective abrasive range of 40–100 mesh which makes it also eligible as potentially reliable and environmentally friendly sustainable abrasive medium for AJM applications. The only concern in both the sands was the percentage of Loss on Ignition (LoI). LoI quantifies how much weight a sample loses when it is heated. This shows how much moisture, organics, or carbonates are removed. LoI levels of roughly 2% are suitable for abrasive grains since larger values mean that there are volatile components that might reduce particle strength and make machining less stable; Chaitanya et al. (2020). In the present study, the slightly higher LoI values in the raw sand samples were taken care of by washing to remove salts and impurities, followed by sun-drying to remove moisture, thereby ensuring consistent abrasive quality. The sand was finally sieved to yield particles between 0.1 and 0.5 mm, with the average particle size obtained as 0.257 mm for Benaulim Beach sand and 0.425 mm for Agonda Beach sand; Sabrinathan et al. (2020).

Table 1. Chemical composition report of Seashore sand of Benaulim beach

Sr. No.	Parameter	Result
1	SiO_2	89.10 %
2	Al_2O_3	2.35 %
3	Fe_2O_3	1.61 %
4	CaO	0.84 %
5	MgO	0.40 %
6	LoI	3.20 %

Table 2. Chemical composition report of Seashore sand of Agonda beach

Sr. No.	Parameter	Result
1	SiO_2	85.23%
2	Al_2O_3	3.65%
3	Fe_2O_3	4.56%
4	CaO	1.12%
5	MgO	0.40%
6	LoI	2.41%

Table 3. Sand particle size distribution report of Seashore sand of Benaulim beach

Sr. No.	Parameter	Result in %
1	-20 mesh +40 mesh	1.80
2	-40 mesh +60 mesh	6.40
3	-60 mesh +80 mesh	41.60
4	-80 mesh +100 mesh	42.90
5	-100 mesh +150 mesh	5.20
6	-150 mesh	2.10

Table 4. Sand particle size distribution report of Seashore sand of Agonda beach

Sr. No.	Parameter	Result in %
1	+10 mesh	1.20
2	-10 mesh +20 mesh	2.40
3	-20 mesh +40 mesh	25.80
4	-40 mesh +60 mesh	18.61
5	-60 mesh +80 mesh	23.25
6	-80 mesh +100 mesh	26.18
7	-100 mesh	2.56

3.2.2 Mild Steel Workpiece Material

The workpiece material used was IS 2062 Grade E250A (Semi-Killed) mild steel plates of size 50 mm × 50 mm × 2 mm. Table 5 shows, chemical composition in mild steel workpiece. Density of mild steel is 7850 kg/m^3 and Yield strength 250 MPa. It is widely used in structural engineering**,** automobile frames, machinery parts, shipbuilding, railways, etc.

Table 5. Percentage chemical composition of mild steel workpiece

C	Si	Mn	P	S	Ni	Cr	Mo	Cu	V	Test Method
0.16	0.015	0.56	0.009	0.004	0.017	0.029	<0.01	0.033	0.001	ASTM E-415:21, IS 8811:1998, JIS G-1253:2002

3.3 Process Parameters and Experimental Design

3.3.1 Control Factors and Response Parameter selection

Study on AJM reveals small set of control variables such as P, d_N, S, A, jet exposure/T, grain size, traverse feed, as the chief determinants of MRR, KTA, depth of cut, Surface finish, etc. This variable controls the air- abrasive distribution and kinematic behaviour of the jet. Higher P and reduced S generally increase material removal efficiency, whereas high A can improve MRR but decrease surface finish; Khan et al. (2008), Kulkarni et al. (2014), Jain et al. (2020), Pandey et al. (2003). Based on these findings, it was decided to take P, d_N, S, A, and T as five control factors in DoE. The standard response parameters adopted were MRR and KTA; Gosh et al. (2019), Dey et al. (2021), Lenin et al. (2019), Uthaykumar et al. (2015), Sumesh et al. (2020), Agarwal et al. (2000).

3.3.2 Design of Experiment (DoE)

Taguchi experimental methodology was adopted to evaluate the effect of control factor settings on MRR and KTA. Taguchi's orthogonal arrays are highly fractional and provide sufficient information with the minimum number of experimental runs thus reducing time and cost of conducting experiments. L_{27} orthogonal array accommodates up to 13 factors at three settings yet limits the test matrix to 27 experimental runs. In AWJM research, BRN et al. (2024) used such an L_{27} scheme to vary S, traverse speed, and A and observed that it provided sufficient information with the minimum number of experiments.

Accordingly, Table 6 and Table 7 depict control factors along with their levels for Benaulim Beach sand and Agonda Beach sand as the abrasive.

Table 6. Control factors with their levels for Benaulim Beach sand as abrasive

	Levels		
	Level 1	Level 2	Level 3
P	5.515 bar	6.5 bar	8 bar
d_N	2 mm	2.5 mm	3 mm
S	2 mm	3 mm	4 mm
A	46.8 g/min	283.8 g/min	470 g/min
T	540 s	600 s	660 s

Table 7. Control factors with their levels for Agonda Beach sand as abrasive

Control Factor	Levels		
	Level 1	Level 2	Level 3
P	5.515 bar	6.5 bar	8 bar
d_N	2 mm	2.5 mm	3 mm
S	2 mm	3 mm	4 mm
A	65g/min	370 g/min	410 g/min
T	540 s	600 s	660 s

The air pressure (P) levels (5.5, 6.5 and 8 bar) were selected in both experiments based on preliminary trials that indicated insufficient material removal below 5 bar and excessive nozzle wear above 8 bar. Stand-off distances (S) of 2–4 mm encompass the range recommended in the literature for cutting mild steel; Khan et al. (2008), Kulkarni et al. (2014), Pandey et al. (2003). In general, cutting efficiency increases with larger abrasive grains up to a point, but particle size is constrained by nozzle diameter. It is recommended to keep abrasive size below about one-third of the nozzle diameter to avoid feed issues; Pawar et al. (2013). Even within this guideline, variations in grit size can alter abrasive flowability and may necessitate adjusting the flow rate or feed mechanism to maintain a stable, clog-free supply; Karkalos et al. (2023). After the feeder had been modified, the coarser Agonda sand, which had an average particle size of 0.425 mm, could only be fed consistently at a reduced abrasive feed rate of 65–410 g/min. The Benaulim sand, which is finer (0.257 mm), flowed smoothly between 46.8 g/min to 470 g/min. These results show the difficulty of moving larger particles and are in accordance with studies that show that enough air entrainment and feed line velocity are important for smooth abrasive feeding without any problems; Karkalos et al. (2023). A total of 27 experiments were conducted using the L_{27} array for each experimental configuration. All machining ensured complete through-holes were obtained on the mild steel plates.

3.3.3 Response Measurements

Response parameters MRR and KTA were determined using the following equations:

$$\text{Material Removal Rate (MRR)} = \frac{(w_i - w_f)}{T} \quad (1)$$

Where,

w_i = Weight of workpiece before machining

w_f = Weight of workpiece after machining

T=Time of jet impingement

$$\text{Kerf Taper Angle (KTA)} = \tan^{-1}\frac{(d_u - d_b)}{2t} \quad (2)$$

Where,

d_u = Upper surface diameter of machined hole

d_b = Lower surface diameter of machined hole

t=Thickness of mild steel plate (Workpiece)

P and A were checked using calibrated pressure gauge (accuracy ±0.05 bar) and random flow measurement (±5 % error). The digital timer and weighing balance were tested to factory calibration standards before each day's work.

The hole sizes were measured with a digital caliper that had a resolution of 0.01 mm and checked with gauge blocks. Written entries from experiments were kept in a lab notebook and then put into Minitab for statistical analysis.

3.4 Statistical Analysis and Evaluation Strategy

3.4.1 Statistical Analysis of the Taguchi Experiments

After completing the Taguchi L_{27} experiments on MRR and KTA, the data were processed in Minitab 2017. Both Benaulim Beach sand and Agonda Beach sand experimental runs data were analysed using Taguchi methods. The effects of the control factors were evaluated from the main-effect plots of the means and signal-to-noise ratios. Response tables for the means and S/N ratios were generated, and the delta (Δ) values were used to rank the relative influence of P, d_N, S, A and T, on MRR and KTA. Furthermore, ANOVA was performed on the data obtained.

3.4.4 Multi-Criteria Decision-Making (MCDM)

To obtain optimum machining conditions, as MRR and KTA are two contradictory response parameters where MRR has to be maximized and KTA has to be minimized, a multi-criteria ranking was performed. MCDM techniques determine the best alternative by considering more than one criterion; Taherdoost et al. (2023). To evaluate each Experimental Run in both experiments, Mixed Aggregation by Comprehensive Normalization Technique (MACONT) MCDM techniques was applied. Weighting schemes favouring accuracy over output were used.

3.4.5 Comparative Benchmarks

As recent AJM data on mild steel with industrial abrasives are limited, we benchmark our results against studies on equivalent ductile steels (e.g., Austenitic SS AISI 304L) under similar AJM conditions for garnet as abrasive material. Therefore, the reported values serve as appropriate scale-based comparators rather than material-matched controls; Thakkar et al. (2013), Tolouei-Rad et al. (2021).

4. AJM Experimentation Results & Analysis

In both sets of experiments, the experimental runs were conducted in a randomized sequence to eliminate bias. For each Experimental Run, the abrasive tank of the AJM machine was filled completely with prepared beach sand. The mild steel workpiece was first weighed on a precision weighing scale to record the initial weight, W_i. The control factors for that run were then set according to the randomized experimental plan: P was adjusted on the regulator, and T was entered into the digital timer. The workpiece was positioned horizontally on the worktable, directly beneath the nozzle at a 90° orientation, and rigidly clamped to prevent vibration or movement during machining. S was adjusted to the prescribed value using a calibrated gauge. After securing the glass door of the enclosure, the machine was switched ON, and the jet continued until the preset T elapsed, at which point the machine automatically stopped. The workpiece was then removed, cleaned thoroughly with rust loosener Weicon contact spray (Germany) to eliminate residual abrasive and oxide films, and dried. The final weight W_f was measured using the same weighing scale. In addition, the upper diameter (d_u) and bottom diameter (d_b) of the machined holes were measured precisely using a digital vernier caliper. These measurements were recorded for each Experimental Run to determine MRR and KTA.

4.1 Experiments using Benaulim Beach Sand as Abrasive

Table 8 shows MRR and KTA achieved by making holes in 2 mm thick mild steel plates by Taguchi L27 OA, 5 factor, and 3 level experimentation. MINITAB software is used for the analysis.

Table 8. Results of Taguchi L_{27} orthogonal array experiments using Benaulim Beach sand

Expt Run.	P (bar)	d_N (mm)	S (mm)	A (g/min)	Wi (g)	T (s)	W_f (g)	d_u (mm)	d_b (mm)	MRR (g/s)	KTA (°)
1	5.515	2	2	46.8	85.683	540	85.548	2.6	2	0.00025	8.53
5	5.515	2.5	3	283.8	85.066	600	84.826	3.8	2.7	0.0004	15.38
9	5.515	3	4	470	83.886	660	83.492	4.42	4.04	0.000597	5.43
10	6.5	2	3	470	83.492	540	83.286	3.6	3	0.000381	8.53

14	6.5	2.5	4	46.8	82.595	600	82.314	3.92	3.5	0.000468	5.99
18	6.5	3	2	283.8	81.568	660	81.221	3.86	3.58	0.000526	4.00
20	8	2	4	283.8	81.05	600	80.83	3.22	2.84	0.000367	5.43
21	8	2	4	283.8	80.83	660	80.616	3.44	1.76	0.000324	22.78
22	8	2.5	2	470	80.616	540	80.367	3.2	3	0.000461	2.86
23	**8**	**2.5**	**2**	**470**	**80.367**	**600**	**79.905**	**3.22**	**3**	**0.00077**	**3.15**
24	8	2.5	2	470	79.905	660	79.536	3.2	3	0.000559	2.86
25	8	3	3	46.8	79.536	540	79.236	4	3.2	0.000556	11.31
26	8	3	3	46.8	79.236	600	78.822	4.2	4	0.00069	2.86
27	8	3	3	46.8	78.822	660	78.501	4	3.62	0.000486	5.43

4.1.1 Taguchi Analysis of MRR vs. P, d_N, S and A

Figures 2 (a) and (b) displays main effect plots of means and signal to noise ratios for response parameter MRR. Table 9 and Table 10 are respective response tables for the "larger-is-better" MRR objective; the signal-to-noise and mean-response tables consistently rank d_N as the most influential factor; its delta value in the means table (0.000251 g/s) is roughly twice that of the next-ranked factor. Larger nozzles deliver higher jet momentum and increase the mass flow of abrasive, leading to a marked rise in MRR. The second- and third-ranked factors are A and P, while S exerts only a modest effect and T has the weakest influence. The means table suggests that to maximize MRR one should select the highest levels of P (8 bar), d_N (3 mm), S (4 mm) and A (470 g/min); the intermediate T (600 s) produced slightly higher MRR than the other time levels. Under this combination the average MRR reaches roughly 0.00054 g/s, whereas the smallest nozzle at low pressure removes less than 0.00030 g/s. In ANOVA analysis control factors P with p-value 0.048, d_N with p-value 0.0001 and A with p-value 0.012 were found to be significant, with the percentage contribution on to MRR by d_N being approximately 66% followed by A at 16%, and P at 10%.

Table 9. Response table of Means for MRR

Level	P (bar)	d_N (mm)	S (mm)	A (g/min)	T (s)
1	0.000408	0.000293	0.000416	0.000435	0.000444
2	0.000421	0.000496	0.000428	0.000384	0.000469
3	0.000503	0.000544	0.000489	0.000514	0.000419
Delta	0.000095	0.000251	0.000073	0.000130	0.000050
Rank	3	1	4	2	5

Table 10. Response table of S/N Ratios for MRR

Level	P (bar)	d_N (mm)	S (mm)	A (g/min)	T (s)
1	-68.58	-70.87	-68.44	-68.01	-67.44
2	-67.75	-66.33	-67.71	-68.43	-67.20
3	-66.35	-65.48	-66.52	-66.24	-68.04
Delta	2.23	5.39	1.92	2.20	0.84
Rank	2	1	4	3	5

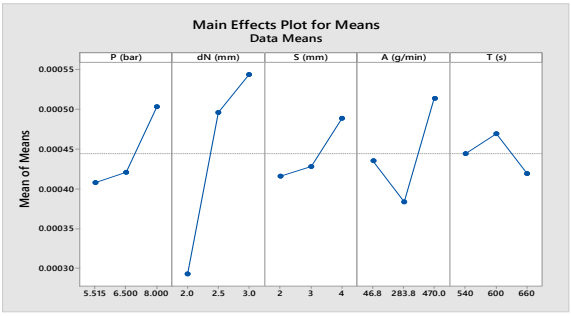

(a)

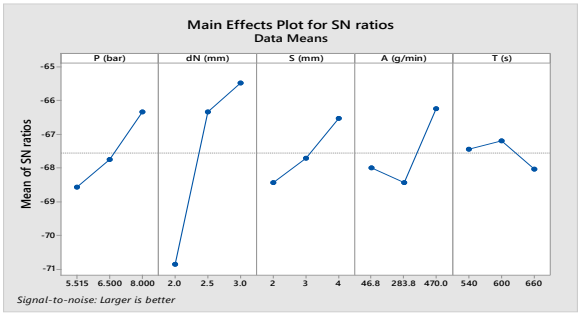

(b)

Figure 2. (a) Main effects plot of means for MRR (b) Main effects plot of S/N ratios for MRR

4.1.2. Taguchi Analysis of KTA vs. P, d_N, S, and A

Figures 3 (a) and (b) displays main effect plots of means and signal to noise ratios for response parameter KTA. Tables 11 and 12 are respective response tables. When KTA is minimized ("smaller-is-better"), the analysis highlights S as the dominant factor, with delta values of 5.93 dB (S/N) and 5.18° (means) far exceeding those of the other variables. A short S (2 mm) minimizes jet divergence and produces the straightest hole walls. d_N and P rank second and third respectively; larger d_N and higher P tend to produce lower KTA by maintaining jet coherence. A and T have comparatively minor effects. The mean responses indicate that the smallest KTA occurs with high P (8 bar), the largest d_N (3 mm), the smallest S (2 mm) and the highest A (470 g/min); KTA decreases slightly with longer T (660 s), although the time effect is the least significant. In this optimal configuration the average KTA drops to about 5.8°, whereas an unfavourable combination of low P, small d_N, and long S yields taper angles above 9°. In ANOVA analysis no control factors were found to be significant on KTA; however, among all the control factors p-value of 0.105 for S was the minimum.

Table 11. Response table of Means for KTA

Level	P (bar)	d_N (mm)	S (mm)	A (g/min)	T (s)
1	9.233	9.001	4.629	6.893	8.461
2	6.758	7.910	9.809	9.431	7.140
3	6.742	5.822	8.296	6.409	7.132
Delta	2.491	3.179	5.180	3.022	1.329
Rank	4	2	1	3	5

Table 12. Response table of S/N Ratios for KTA

	P (bar)	d_N (mm)	S (mm)	A (g/min)	T (s)
1	-18.34	-17.73	-12.56	-16.16	-17.28
2	-15.81	-16.07	-18.49	-17.17	-15.57
3	-14.11	-14.47	-17.22	-14.93	-15.41
Delta	4.23	3.27	5.93	2.23	1.87
Rank	2	3	1	4	5

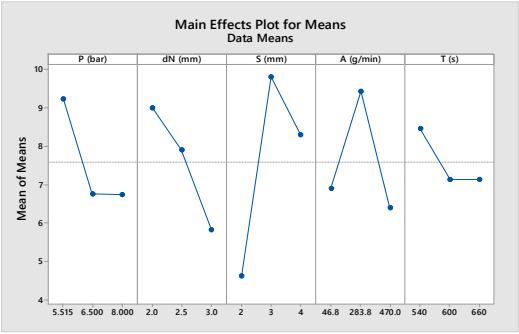

(a)

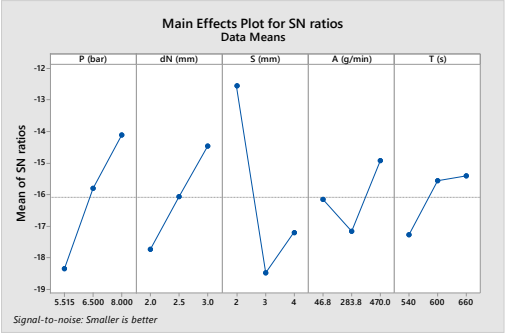

(b)

Figure 3. (a) Main effects plot of means for KTA (b) Main effects plot of S/N ratios for KTA

4.2 Experiments using Agonda Beach Sand as Abrasive

Table 13 shows MRR and KTA achieved by making holes in 2 mm thick mild steel plates by Taguchi L_{27} OA, 5 factor and 3 level experimentation. MINITAB software is used for the analysis.

Table 13. Results of Taguchi L_{27} orthogonal array experiments using Agonda Beach sand

Expt Run.	P (bar)	d_N (mm)	S (mm)	A (g/min)	Wi (g)	T (s)	W_f (g)	d_u (mm)	d_b (mm)	MRR (g/s)	KTA (°)
1	5.515	2	2	65	540	50.735	50.66	2.34	2.15	0.0001	2.72
4	5.515	2.5	2	370	540	51.11	51.01	2.74	2.65	0.0002	1.29
7	5.515	3	2	410	540	48.816	48.620	3.51	3.35	0.0004	2.29
8	5.515	3	3	65	600	49.52	49.269	3.50	3.34	0.0004	2.29
9	5.515	3	4	370	660	49.071	48.816	3.82	3.60	0.0004	3.15
10	6.5	2	2	370	540	51.58	51.54	2.21	2.20	0.0001	0.14
12	6.5	2	4	65	660	51.71	51.58	2.96	2.74	0.0002	3.15
13	6.5	2.5	2	410	540	47.870	47.761	2.72	2.45	0.0002	3.86

16	6.5	3	2	65	540	52.14	51.99	3.36	3.20	0.0003	2.29
20	8	2	3	65	600	51.89	51.71	2.48	2.45	0.0003	0.43
21	8	2	4	370	660	51.99	51.89	2.95	2.77	0.0002	2.58
22	8	2.5	2	65	540	52.610	52.495	2.78	2.59	0.0002	2.72
24	8	2.5	4	410	660	48.226	47.870	2.95	2.43	0.0005	7.41
25	**8**	**3**	**2**	**370**	**540**	**53.03**	**52.80**	**3.54**	**3.52**	**0.0004**	**0.29**
26	8	3	3	600	600	48.411	48.226	3.48	3.19	0.0003	4.15
27	8	3	4	65	660	52.80	52.610	3.45	3.31	0.0003	2.00

4.2.1 Taguchi Analysis of MRR vs. P, d_N, S, and A

Figures 4(a) and 4(b) display the main effect plots of means and signal-to-noise ratios for the MRR response when using Agonda sand. Tables 14 and 15 list the corresponding response tables for the "larger-is-better" objective. Both the S/N and mean-response analyses consistently rank d_N as the dominant factor. Its delta value in the means table (0.00016 g/s) is nearly twice that of the next-ranked factor, P. A larger d_N increases jet momentum and abrasive mass flow, thus markedly increasing MRR. P is the second-most influential factor; higher pressures accelerate particles and raise MRR. S, T, and A have comparatively less effects. The mean responses suggest that to maximize MRR, best settings are P (8 bar), d_N (3 mm), S (4 mm), A (410 g/min) and T (660 s). Under this combination the average MRR approaches 0.00034 g/s, whereas the smallest d_N at low pressure removes roughly 0.00018 g/s. ANOVA results corroborate the dominance of d_N (p= 0.003) with moderate contributions from P (p= 0.089) while A, S and T show negligible significance.

Table 14. Response table for Means for MRR

Level	P (bar)	d_N (mm)	S (mm)	T (s)	A (g/min)
1	0.000250	0.000178	0.000231	0.000231	0.000250
2	0.000218	0.000260	0.000268	0.000268	0.000255
3	0.000308	0.000337	0.000276	0.000276	0.000271
Delta	0.000090	0.000160	0.000044	0.000044	0.000021
Rank	2	1	3.5	3.5	5

Table 15. Response table for S/N Ratios for MRR

Level	P (bar)	d_N (mm)	S (mm)	T (s)	A (g/min)
1	-72.72	-75.53	-73.66	-73.66	-72.46
2	-73.84	-72.26	-71.81	-71.81	-72.85
3	-70.81	-69.58	-71.91	-71.91	-72.06
Delta	3.03	5.96	1.85	1.85	0.79
Rank	2	1	3.5	3.5	5

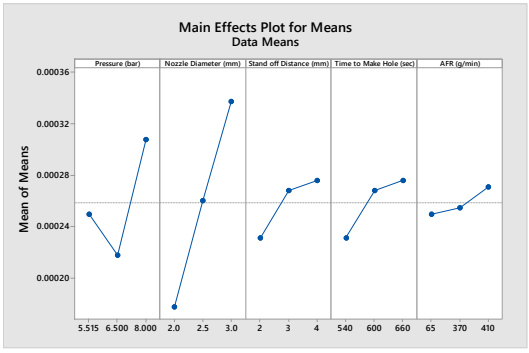

(a)

Figure 4. (a) Main effects plot of means for MRR

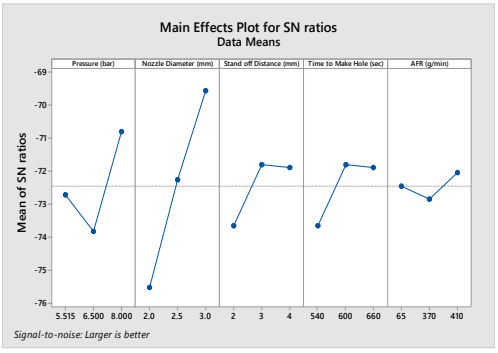

(b)

(b) Main effects plot of S/N ratios for MRR

4.2.2. Taguchi Analysis of KTA vs. P, d_N, S, and A

Figures 5(a) and 5(b) show the main effect plots for KTA using Agonda sand. Tables 16 and 17 present the mean and S/N response tables for the "smaller-is-better" KTA objective. The analysis identifies S and T as the most influential factors controlling KTA. Their delta values (1.792° in the means table and 8.497 dB in the S/N table) exceed those of P, d_N, and A. S of 2 mm and T of 540 s keeps the jet focused and minimizes divergence, producing the smallest KTA. d_N, and A also affect KTA. P has the least impact on KTA. The mean responses therefore indicate that the optimal configuration for minimizing KTA is high P (8 bar), small d_N (2 mm), short S (2 mm), medium A (370 g/min) and T (540 s). Under these conditions the average KTA can be reduced to 2.3°, whereas an unfavourable combination of

long S, T, and large d_N produces KTA exceeding 5°. ANOVA confirms the significance of S (p= 0.003354), T (p= 0.003354), A (p= 0.0043), and P (p= 0.0062) on KTA.

Table 16. Response table of Means for KTA

Level	P (bar)	d_N (mm)	S (mm)	T (s)	A (g/min)
1	3.116	2.369	1.877	1.877	2.561
2	2.957	3.906	3.195	3.195	2.242
3	2.668	2.465	3.669	3.669	3.938
Delta	0.448	1.537	1.792	1.792	1.696
Rank	5	4	1.5	1.5	3

Table 17. Response table of S/N Ratios for KTA

Level	P(bar)	d_N (mm)	S (mm)	T (s)	A (g/min)
1	-9.256	-4.282	-2.244	-2.244	-7.029
2	-7.237	-11.03	-8.694	-8.694	-3.623
3	-5.187	-6.373	-10.741	-10.741	-11.028
Delta	4.069	6.744	8.497	8.497	7.405
Rank	5	4	1.5	1.5	3

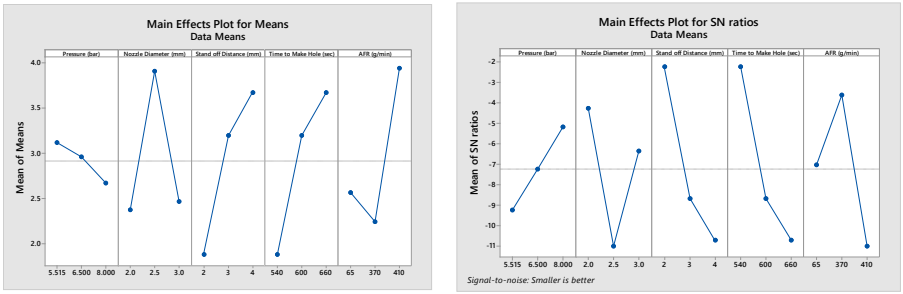

(a) (b)

Figure 5. (a) Main effects plot of means for KTA (b) Main effects plot of S/N ratios for KTA

5. Comparative Performance Analysis of Benaulim Beach Sand and Agonda Beach Sand as Abrasive

5.1 Overall comparison of MRR and KTA

Table 18. Comparison of MRR and KTA for Benaulim and Agonda Beach sand

Sand (abrasive)	Mean MRR (g/s)	Min MRR (g/s)	Max MRR (g/s)	Mean KTA (°)	Min KTA (°)	Max KTA (°)
Benaulim beach sand	0.000444	0.000198	0.000770	7.58	2.86	22.78
Agonda beach sand	0.000263	0.000100	0.000500	2.91	0.14	7.41

Table 18 shows that Benaulim Beach sand consistently produced a higher MRR, around an average 70 % higher, but also resulted in KTA about 2–3 times larger than those achieved with Agonda Beach sand, indicating lower cut accuracy.

5.2 Control Factor-Level comparison

Table 19 below summarizes the mean MRR and KTA obtained at different levels of the three common control factors (P, d_N and S) in the Taguchi experiments. The ratios/differences highlight how much higher the Benaulim results were compared with the Agonda results.

Table 19. Comparison of mean MRR and mean KTA obtained at three levels of control factors using Benaulim (B1) and Agonda (A1) Beach sand

Factor & level	Mean MRR (Benaulim) (g/s)	Mean MRR (Agonda) (g/s)	MRR ratio B1/A1	Mean KTA (Benaulim) (°)	Mean KTA (Agonda) (°)	KTA difference B1–A1 (°)
(P)						
5.515 bar	0.000408	0.000256	1.59	9.23	3.12	+6.12
6.50 bar	0.000421	0.000233	1.81	6.76	2.96	+3.80
8.00 bar	0.000503	0.000300	1.68	6.74	2.67	+4.07
(d_N)						
2.0 mm	0.000293	0.000189	1.55	9.00	2.37	+6.63
2.5 mm	0.000496	0.000256	1.94	7.91	3.91	+4.00

3.0 mm	0.000544	0.000344	1.58	5.82	2.47	+3.36
(S)						
2 mm	0.000416	0.000233	1.79	4.63	1.88	+2.75
3 mm	0.000428	0.000267	1.60	9.81	3.20	+6.61
4 mm	0.000489	0.000289	1.69	8.30	3.67	+4.63

From the table it can be inferred that:

- MRR: For all factor levels, Benaulim sand produced a higher MRR than Agonda sand. Increasing P and d_N generally increased MRR for both sands. The ratio of Benaulim MRR to Agonda MRR was between 1.5 and 2.0 across most levels, with the greatest relative increase at P (6.50 bar) and d_N (2.5 mm).
- KTA: Agonda sand provided significantly lower KTA (better precision) at every level. KTA decreased with increasing d_N for both sands. The highest KTA difference occurred at S (3 mm), where Benaulim's KTA was over 6° larger than Agonda's.
- Statistical analysis revealed that the nozzle diameter had the greatest impact on both MRR and KTA when machining with Benaulim sand, especially when increasing d_N from 2 mm to 3 mm. For Agonda sand, d_N predominantly affected MRR, whereas KTA was more sensitive to S and T.
- An increased MRR; however, a larger KTA, is exhibited by Benaulim sand, which subsequently decreases dimensional accuracy. On the other hand, a slower MRR while achieving a considerably lower KTA is exhibited by Agonda sand, making it more appropriate for applications that require precise cuts. Selecting a larger $d_{N,}$ and higher P can improve MRR for both abrasives, but at the cost of KTA for Benaulim Beach sand.

Figure 6 and 7 illustrate how the mean MRR and KTA vary with the main control factors for each sand. The groupings highlight the consistently higher MRR and larger KTA of Benaulim Beach sand compared with Agonda Beach sand.

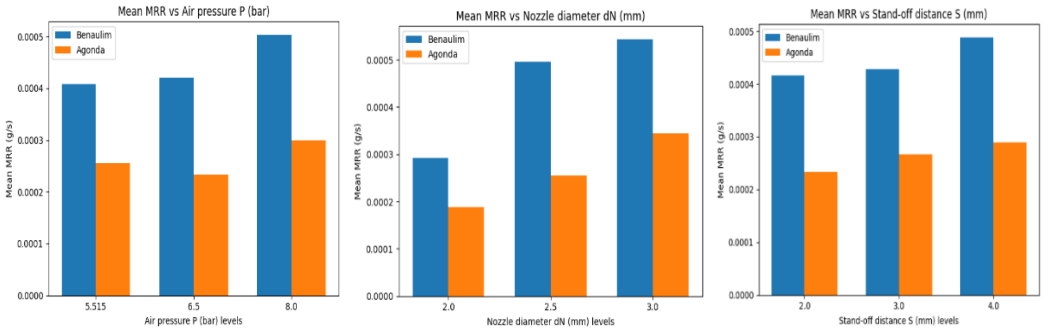

(a) (b) (c)

Figure 6. Mean MRR vs. (a) Air pressure (P) (b) Nozzle diameter(d_N) (c) Stand-off Distance(S)

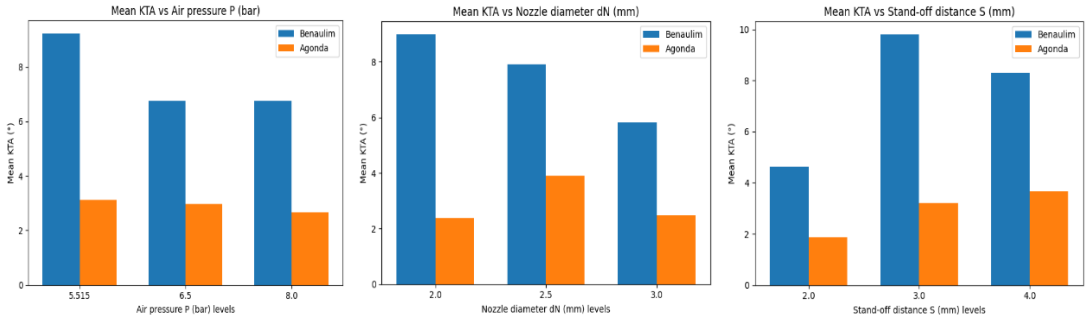

(a) (b) (c)

Figure 7. Mean KTA vs. (a) Air pressure (P) (b) Nozzle diameter(d_N) (c) Stand-off Distance(S)

6. Multi-Criteria Decision-Making (MCDM) Technique

To resolve the conflicting responses (high MRR versus low KTA) produced by the Taguchi L_{27} experiments, this study used Mixed Aggregation by Comprehensive Normalization Technique (MACONT), a recently developed MCDM method that tackles two fundamental challenges in multi-criteria analysis, i.e., normalization and aggregation. In

conventional MCDM methods, using a single normalization technique can distort data and produce contradictory rankings. According to Wen et al. (2020), the majority of MCDM method approaches do not use mixed aggregation functions and numerous normalizing strategies at the same time, which results in deviations and inaccurate conclusions. To solve this, MACONT applies two mixed aggregation operators and presents a thorough normalizing method based on criteria types.

6.1. Steps in Getting Optimum Solution

i. Normalize each Experimental Run's MRR and KTA using three normalization techniques-linear sum-based, linear ratio-based and linear max–min.

If a_{ij} represents the performance value of the i[th] alternative under the j[th] criterion, where i=1,2,3, …, n and j= 1, 2, 3, …, m

$$\bar{a}_{ij}^1 = \frac{a_{ij}}{\sum_{i=1}^m a_{ij}} \text{ for MRR (benefit Criteria),}$$
$$\bar{a}_{ij}^1 = \frac{1}{a_{ij}} / \sum_{i=1}^m \frac{1}{a_{ij}} \text{ for KTA (Cost Criteria),} \quad \text{Linear sum-based normalization} \quad (1)$$

$$\bar{a}_{ij}^2 = \frac{a_{ij}}{max_i\, a_{ij}} \text{ for MRR (benefit Criteria),}$$
$$\bar{a}_{ij}^2 = \frac{min_i\ a_{ij}}{a_{ij}} \text{ for KTA (Cost Criteria),} \quad \text{Linear ratio-based normalization} \quad (2)$$

$$\bar{a}_{ij}^3 = \frac{(a_{ij} - min_i\, a_{ij})}{(max_i\, a_{ij} - min_i\ a_{ij})} \text{ for MRR (benefit Criteria),}$$
$$\bar{a}_{ij}^3 = \frac{(a_{ij} - max_i\, a_{ij})}{(min_i\, a_{ij} - max_i\ a_{ij})} \text{ for KTA (Cost Criteria)} \quad \text{Linear max-min normalization} \quad (3)$$

ii. Synthesize these normalized values with weights λ and μ to reduce the influence of scale differences

$$\bar{a}_{ij} = \lambda \bar{a}_{ij}^1 + \mu \bar{a}_{ij}^2 + (1 - \lambda - \mu)\bar{a}_{ij}^3 \quad (4)$$

Where $0 \leq \lambda, \quad \mu \leq 1$,

iii. A virtual reference alternative is to be generated from the average performance on each criterion, and the distances between each run and the reference are aggregated using a compensatory operator (arithmetic–geometric combination) and a non-compensatory operator (best-worst difference), yielding two subordinate scores.

Virtual reference alternatives:

The weighted arithmetic difference $\rho_i = \sum_{j=1}^n w_j \left(\bar{a}_{ij} - \bar{a}_j\right)$ (5)

A weighted geometric ratio $Q_i = \frac{\prod_{\gamma=1}^n (\bar{a}_j - \bar{a}_{ij})^{w_j}}{\prod_{\eta=1}^n (\bar{a}_{ij} - \bar{a}_j)^{w_j}}$ (6)

Where,

w_j = The weights of criteria such that $\sum_{j=1}^n w_j = 1$

$\gamma = 1,2, \ldots\ldots, n$ represent the part of the criteria where $\bar{a}_{ij} < \bar{a}_j$

$\eta = 1,2, \ldots\ldots, n$ represent the part of the criteria where $\bar{a}_{ij} > \bar{a}_j$

δ and ϑ are preference parameters where $0 \leq \delta, \vartheta \leq 1$

Subordinate comprehensive score for alternatives $S_1(x_i)$ and $S_2(x_i)$

$$S_1(x_i) = \delta\left(\frac{\rho_i}{\sqrt{\sum_{i=1}^m (\rho_i)^2}}\right) + (1-\delta)\left(\frac{Q_i}{\sqrt{\sum_{i=1}^m (Q_i)^2}}\right), i = 1,2, \ldots, m \quad (7)$$

$$S_2(x_i) = \vartheta max_j \left(w_j\left(\bar{a}_{ij} - \bar{a}_j\right)\right) + (1-\vartheta) min_j \left(w_j\left(\bar{a}_{ij} - \bar{a}_j\right)\right), i = 1,2, \ldots, m \quad (8)$$

iv. Normalize these scores and combine to produce a final comprehensive score for each run, and the alternative with the highest score is selected as the optimum.

$$S(x_i) = \frac{1}{2}\left(S_1(x_i) + \frac{S_2(x_i)}{\sqrt{\sum_{i=1}^m \left(S_2(x_i)\right)^2}}\right), i = 1,2, \ldots, m \quad (9)$$

6.2 Selection of $w_j, \lambda, \mu, \delta, \vartheta$

As response parameters taken in this work are:

- Material removal rate (MRR) - a benefit criterion (higher values improve productivity).
- Kerf taper angle (KTA) - a cost criterion (smaller values improve dimensional accuracy).

These responses represent conflicting objectives. For mass production or general manufacturing weights of MRR: KTA trade-off is often balanced (e.g., 50:50 or 60:40) because productivity and tolerances are equally important. In precision industries such as aerospace, tool-and-die, biomedical, etc., dimensional accuracy and surface integrity are far more important than rate of production. Studies on wire-EDM and abrasive water-jet machining often assign much higher weights to KTA and surface roughness than to MRR. For example, AHP-based studies on Wire EDM weight assigned to MRR was 10 % and 90 % to Surface finish and KTA, while other authors apply KTA:MRR ratios of 70:30 or 80:20 when dimensional accuracy is mission-critical. Entropy-based weighting of KTA and Surface roughness has also been reported with nearly equal weights (0.50 each) under neutral conditions; Kumar et al. (2021), Lin et al. (2022), Kharat et al. (2025), Wen et al.(2020).Based on this evidence, we adopt a moderate quality bias for the present work considering KTA is critical for precision however, high productivity is still desirable. Thus, the following criterion weights for all MCDM methods are recommended (Table 20).

Table 20. Criterion weights for all MCDM methods

Response Parameter	Weight W_j	Remarks
MRR	0.4	The productivity is less critical than dimensional accuracy
KTA	0.6	KTA directly influences dimensional accuracy and fit. Precision industries emphasise small taper angles; weighting KTA at 0.60 prioritises quality and also acknowledges the need for reasonable MRR. Extreme quality-biased ratios (e.g., 0.8-0.9) unduly penalise experiments with excellent MRR.

- λ controls the influence of the sum-based normalization. Larger the λ greater importance given to the relative contribution of each alternative's performance to the total.
- μ weights the ratio-based normalization, which highlights the best performances by scaling each value against the column maximum (benefit) or minimum (cost).
- The remaining weight (1- λ - μ) is assigned to the max–min normalization, which preserves the range of each criterion.

In this case we used balanced values so that no single normalization biases the results. Equal weights ($\lambda = \mu = 1/3$). Following this recommendation, we adopt:

- $\lambda = 0.33$ $\mu = 0.33$ $(1- \lambda - \mu) = 0.34$

This slightly favours the max–min normalization, which increases comparability when criteria have very different scales (MRR vs. KTA).

- Aggregation parameters (δ and ϑ)

1. compensatory aggregation $S_1(x_i)$ blends the weighted arithmetic difference ρ_i and a weighted geometric ratio Q_i
   - δ $(0 \leq \delta \leq 1)$ determines the importance between overall performance ρ and individual dominance Q. A higher δ favours alternatives with good overall averages, while a smaller value highlights alternatives with standout performance in one or a few criteria.
2. Non-compensatory aggregation $S_2(x_i)$ blends the best and worst weighted deviations for each alternative.
   - ϑ balances the emphasis between the best criterion (higher ϑ) and the worst criterion (lower ϑ).
     As there are no strong preferences, the original MACONT study recommends using neutral settings (δ =0.5, ϑ =0.5) so that neither component dominates; Wen et al. (2020). As the goal here is to rank experiments without bias and to respect both overall quality and standout performance, so the neutral setting was adopted. These weights and parameters ensure that the MCDM rankings reflect both industrial priorities and methodological balance.

6.3 MACONT Analysis Results and Discussion

Tables 20, 21 and 22 show the scores obtained using MACONT for the 27 experimental runs performed with Benaulim and Agonda Beach sands, respectively. The MACONT method identified Run 23 (P (8 bar), d_N (2.5 mm), S (2 mm),

A (470 g/min), and T (600 s)) as the optimal Run, producing an MRR of 0.00077 g/s and a KTA of 3.15°. for Benaulim Beach sand with its finer particles (~0.257 mm) as abrasive. Runs employing 3 mm d_N also exhibited favourable KTA (2.86°–4.00°) but slightly lower MRRs. In contrast, large S and small d_N increased the KTA dramatically (up to 22.78°) and reduced the MRR. These findings indicate that for Benaulim sand d_N is the dominant factor affecting both productivity and accuracy.

Agonda Beach sand, with its coarser particles (~0.425 mm), shows a different performance behaviour. The optimal Run 25 (P (8 bar), d_N (3 mm), S (2 mm), A (370 g/min), and T (540 s)) produced an MRR of 0.00043 g/s alongside an exceptionally low KTA of 0.284°. This confirms that coarser abrasives favour accuracy over material removal. Runs with reduced P or increased S increased the KTA and decreased MRR.

Table 21. Best 5 Rankings of Experimental runs using Benaulim Beach sand as abrasive

Expt. Run	MRR (g/s)	KTA (°)	ρ	Q	$S_1(X)$	$S_2(X)$	S(X)	Rank
9	0.000597	5.43	0.265	0.295	0.588	0.2938	0.853	4
18	0.000526	4	0.262	0.292	0.58	0.2899	0.844	5
23	**0.00077**	**3.15**	**0.327**	**0.329**	**0.689**	**0.3444**	**1**	**1**
24	0.000559	2.86	0.281	0.303	0.612	0.3058	0.89	3
26	0.00069	2.86	0.312	0.32	0.664	0.3321	0.964	2

Table 22. Best 5 Rankings of Experimental runs using Agonda Beach sand as abrasive

Expt Run	MRR (g/s)	KTA (°)	ρ	Q	$S_1(X)$	$S_2(X)$	S(X)	Rank
7	0.000363	2.291	0.221	0.27	0.513	0.257	0.748	4
8	0.000418	2.291	0.237	0.28	0.541	0.271	0.788	3
11	0.000152	4.004	0.115	0.189	0.292	0.146	0.45	25
20	0.0003	0.43	0.254	0.286	0.562	0.281	0.821	2
25	**0.000426**	**0.286**	**0.294**	**0.311**	**0.635**	**0.318**	**0.922**	**1**
27	0.000288	2.005	0.208	0.26	0.485	0.242	0.711	5

Overall, it can be inferred that Agonda beach sand yields superior cutting accuracy but lower productivity relative to Benaulim Beach sand. These results illustrate an inherent trade-off: finer particles of beach sand enhance MRR at the expense of KTA, whereas coarser particles improve KTA but reduce MRR.

7. Benchmarking the performance of Benaulim and Agonda Beach Sand with Garnet Abrasive

This benchmarking test as shown in Table 23 compares the performance of beach sands in air-driven AJM to published results for garnet-based abrasive machining. Thakkar et al. (2013) and Tolouei-Rad et al. (2021) examined mild steel and AISI 304L stainless steel, employing 80 mesh garnet at AWJM conditions, typically at pressures about 275–290 MPa. In the present study though air at pressures between 5.5 and 8 bar was used for machining; the existing literature would serve as a significant reference for evaluating performance trends.

Table 23. Comparative benchmarking of beach sand abrasive results with garnet abrasive in AJM

Study/abrasive	Process medium & pressure	Abrasive/ mesh	Feed/flow ranges	Reported KTA (°)	Reported MRR
Thakkar et al. (2013)	AWJM at 290 MPa	Garnet, #80	Traverse speed 250 - 350 mm/min, A:250 - 350 g/min, S: 2 - 10 mm	Not available	0.56 – 0.78 g/s (thickness of mild steel workpiece :10 mm)

					High water pressure, fine garnet, higher traverse speed and abrasive flow produced high MRR.
Tolouei-Rad et al. (2021)	AWJM at 275 MPa	Garnet, #80	Traverse speed 90 – 150 mm/min, A: 300 g/min S:1.5 mm	0.825 - 1.55 (thickness of Austenitic SS AISI 304L workpiece: 4 mm)	4.56 g/s maximum for 4mm thick workpiece.
Benaulim Beach sand	Air AJM at 5.5–8 bar	Sand, (~#60)	A:46.8–470 g/min, S: 2 - 4 T: 540–660 s	2.86–22.78	Finer sand gave the highest MRR of 0.00077 g/s
Agonda Beach sand	Air AJM at 5.5–8 bar	Sand, (~#40)	A:65–410 g/min, S: 2 – 4 mm T: 540–660 s	0.143-7.407	Coarser particles reduced MRR (max ≈ 0.000539 g/s)

7.1 Benchmarking Discussion

While garnet-based AWJM achieves much higher MRR due to its immense hydraulic power, the present air-driven AJM process demonstrates comparable kerf quality at vastly reduced energy input. The Agonda Beach sand, though coarser, delivered a remarkably low KTA of 0.28°, matching the dimensional precision achieved with garnet in certain low-pressure AJM studies. Conversely, the finer Benaulim Beach sand achieved roughly 0.00077 g/s MRR, offering a practical trade-off between productivity and accuracy.

A direct experimental comparison using standard 80 mesh garnet under identical AJM conditions is planned as future work to validate these literature-based benchmarks. Preliminary expectations suggest that garnet would enhance MRR but marginally increase KTA, reinforcing the distinct trade-off between removal rate and precision.

7.2 Merits of Local Beach Sands versus Garnet

- Sustainability and cost: Garnet is mined and processed, and abrasives typically account for over 50 % of water-jet machining costs. In this study processing done on the locally sourced sand was only simple washing and sieving and therefore it reduces both environmental impact and consumable cost.
- Comparable accuracy at lower energy: An optimal kerf taper of roughly 0.28° was achieved by using the Agonda sand while being driven by air at only 8 bar. This accuracy is comparable to that obtained with garnet under pressures of several hundred megapascals, demonstrating that carefully prepared natural sand can produce precise cuts without extreme pressures.
- Trade-off between productivity and precision: A clear trade off emerged: the coarse Agonda sand provided a favourable KTA but removed only about 0.00043 g/s MRR, whereas the finer Benaulim sand increased the MRR to around 0.00077 g/s at the cost of a much KTA (approximately 3°). AWJM with garnet can simultaneously deliver high MRR and low KTA, but at much higher energy consumption and equipment cost.
- Process adaptability: The AJM setup drilled through holes in 2 mm thick mild steel plates in roughly 9–11 minutes using only compressed air. Even though this is slower than AWJM, the main advantage is system's low cost and portability, which benefits small workshops or remote locations where high pressure water systems are impractical.
- Limitations: Natural sands vary slightly in composition and grain shape between batches and thus introduces variability. Therefore, sand consistency and reusability will be taken into consideration in future optimization.

8. Conclusion

Based on the results of this investigation, it can be concluded that carefully prepared beach sand from the Goan coast can serve as a viable abrasive medium for air driven AJM of mild steel. Experiments conducted on a custom built AJM rig using Taguchi's L27 design demonstrated that five process variables, P, d_N, S, A and T, strongly influence both MRR and KTA. Statistical analyses and multi criteria optimization showed that d_N had the greatest effect on MRR, while S and A were more critical for controlling KTA. Benaulim Beach sand, the finer of the two sands, achieved the highest MRR (0.00077 g/s) under optimum conditions, whereas the coarser Agonda Beach sand yielded an exceptionally low KTA (0.284°) with a modest MRR. These results illustrate that particle size distribution directly governs the balance between productivity and dimensional accuracy. When benchmarked against published AWJM studies using garnet, which operate at pressures two orders of magnitude higher and employ commercially mined abrasives, the prepared sands delivered comparable or superior kerf quality despite the much lower jet energy. Moreover, all experiments were done at modest pressures of 5.5–8 bar using air as the carrier fluid; this contrasts

favourably with the 250–350 MPa pressures commonly reported in AWJM of low alloy steels, where high traverse speed and abrasive flow improve material removal at the expense of taper. The present work therefore demonstrates that sustainable abrasives can reduce the environmental impact and operating costs of AJM while still producing precision cuts. Replacing mined abrasives with locally sourced sand reduces transportation and processing, and the simplicity of the air driven system makes it suitable for small workshops, especially in coastal regions where the raw material is plentiful.

In practical terms, the Agonda Beach sand's low KTA makes it suitable for precision drilling or engraving, while Benaulim Beach sand's higher MRR can be favored for rapid material removal. Locally sourced sand only needs simple washing and sieving, making it a more sustainable and lower-impact alternative to mined abrasives. This study demonstrates that adequately processed beach sand can compete with commercial garnet in low-pressure AJM. It also uses MCDM methods to find settings that maximize MRR while minimizing KTA.The results show that community-based abrasive manufacture is possible and promote the search for other natural or recycled materials that are both cost-effective and good for the environment. In the future, research will directly compare these sands to garnet in the same AJM settings, test their reusability, and investigate long-term impacts like wear on the nozzle and exposure to silica in the air. Also extend the approach to other ductile and brittle materials, thereby broadening the scope of eco efficient non-traditional machining.

References:

Abdelnasser, E. S., Elkaseer, A., & Nassef, A., Modeling and experimental investigation of abrasive jet machining of glass using sand as abrasive, *PSERJ, 2016.*

Agrawal, V. and Choudhury, S. K., A study on the performance of alternative abrasives in abrasive jet machining, Conference *on Materials Processing Technology*, pp. 3–7, 2000.

Anjaneyulu, B., D. Harshavardhan, R. Meenakshi Reddy, T. Hariprasad, and M. Usha Rani., Exploration of machining parameters by using Taguchi technique on MAAJDM, *Materials Today: Proceedings* (2023).

ASTM International., *ASTM D7348–13: Standard test methods for loss on ignition (LOI) of solid combustion residues*. West Conshohocken, PA: ASTM International, 2013.

Bayraktar, Ş., Sustainable abrasive jet machining, *Sustainable abrasive jet machining* (book chapter), 2022.

Chaitanya, A. K., Babu, D. K. and Kumar, K. G., Experimental study on surface roughness by using abrasive jet machine, *Materials Today: Proceedings*, pp. 453–457, 2020.

Chatterjee, S., & Chakraborty, S., Optimization of abrasive water jet machining processes using mixed aggregation by comprehensive normalization technique (MACONT) under single-valued neutrosophic fuzzy environment, *Sādhanā, 50*, Article 198, 2025.

Chotaliya, J. N., Waghela, H. B., Gavhane, A. T. and Nikam, S. S., Design, fabrication and analysis of an abrasive jet machining system, *International Journal of Engineering and Advanced Technology Conference*, pp. 2713–2718, 2020.

Dey, S. and Mitra, S., Optimization of AWJM process using hybrid MCDM: GRA and EDAS, *Materials Today: Proceedings*, pp. 1013–1018, 2021.

Ghosh, S. and Bandyopadhyay, A., Multi response optimization in micro AJM using Taguchi GRA, PROMETHEE, *Materials Today: Proceedings*, pp. 289–295, 2019.

Gupta, A., Performance optimization of abrasive fluid jet for completion and stimulation of oil and gas wells, *Journal of Energy Resources Technology*, 134(2):021001– 021001, 2012.

Gupta, K., Developments in abrasive water jet machining of nonmetals, *Politeknologi journal*,2024.

Hashish., Abrasive waterjet machining, *Materials*, *17*(13), 3273, 2024.

Jain, R. K. and Sidhu, T. S., Parametric study of abrasive jet machining for sustainable manufacturing, *Materials Today: Proceedings*, pp. 2069–2074, 2020.

Karkalos, N. E. and Karmiris Obratński, P., Determination of the feasibility of using eco-friendly walnut shell abrasive particles for pocket milling of titanium workpieces by abrasive waterjet technology, *Metals Conference*, 2023.

Karkalos, N. E., & Karmiris-Obratański, P., Determination of the feasibility of using eco-friendly walnut shell abrasive particles for pocket milling of titanium workpieces by abrasive waterjet technology, *Metals, 13*(10), Article 1645, 2023.

Karkalos, Nikolaos E., Panagiotis Karmiris-Obratański, and Rafał Kudelski., An experimental investigation into the potential of employing mixed eco-friendly abrasives during AWJ milling of nickel-based superalloy, *The International Journal of Advanced Manufacturing Technology* 134, no. 11: 5143-5158, 2024.

Kawecka, Elzbieta, Andrzej Perec, and Aleksandra Radomska-Zalas., Use of the simple multicriteria decision-making (MCDM) method for optimization of the high-alloy steel cutting process by the abrasive water jet, *Spectrum of Mechanical Engineering and Operational Research* 1, no. 1: 111-120, 2024.

Khan, A. A., & Haque, M. M., Performance of different abrasive materials during abrasive water jet machining of glass, *Journal of materials processing technology*, *191*(1-3), 404-407, 2007.

Khan, A. A., A study of abrasive jet machining in controlled machining environment, *International Conference on Machine Tools and Manufacture*, pp. 1214–1223, 2008.

Kharat, Dipak P., M. P. Nawathe, and C. R. Patil., Prioritization of Critical Process Parameters in Wire Electrical Discharge Machining Using Analytic Hierarchy Process: A Comprehensive Analysis, *Metallurgical and Materials Engineering*, 1067-1081, 2025

Kulkarni, A. V. and Rathod, P. P., Analysis of process parameters in abrasive jet machining, *Procedia Materials Science Conference*, pp. 2562–2567, 2014.

Kumar, Raman, Sehijpal Singh, Paramjit Singh Bilga, Jasveer Singh, Sunpreet Singh, Maria-Luminiţa Scutaru, and Cătălin Iulian Pruncu., Revealing the benefits of entropy weights method for multi-objective optimization in machining operations: A critical review, *Journal of materials research and technology,* 10: 1471-1492, 2021

Lenin Raj, A. and Rajadurai, A., Investigation of deep hole drilling in Ti-6Al-4V alloy using abrasive water jet machining, *Materials Research Express Conference*, 2019.

Lin, Yongchuan, Jiyang Ma, Debin Lai, Jingru Zhang, Weizhu Li, Shengzhu Li, and Shengjian He., Multi-response optimization of process parameters in nitrogen-containing gray cast iron milling process based on application of non-dominated ranking genetic algorithm, *Heliyon* 8, no. 11, 2022.

Palaniyappan, S., Annamalai, V. E., & Kaliyamoorthy, R., Sustainable application of grinding wheel waste as abrasive for abrasive water jet machining process, *Journal of Cleaner Production, 261*, Article 121225, 2020.

Pandey, A. K. and Shan, H. S., Cutting performance of abrasive jet machining on glass and metals, *International Conference on Advanced Manufacturing Technology*, pp. 1–4, 2003.

Pawar, N. S., Lakhe, R. R. and Shrivastava, R. L., A comparative experimental analysis of sea sand as an abrasive material using silicon carbide and mild steel nozzle in vibrating chamber of abrasive jet machining process, *International Conference on Scientific and Research Publications*, pp. 250–253, 2013.

Sabarinathan, P., Annamalai, V. E. and Rajkumar, K., Sustainable application of grinding wheel waste as abrasive for abrasive water jet machining process, *Conference on Cleaner Production*, 2020.

Sumesh, K. and Kanthavel, K., Abrasive water jet machining on hybrid natural fiber composites using Taguchi method, *Materials Research Express Conference*, country, 2020.

Taherdoost, H. and Madanchian, M., Using PROMETHEE method for multi-criteria decision making: applications and procedures, *Iris Conference on Economics & Business Management*, *1*(1)

Thakkar, P., Prajapati, P., & Thakkar, S. A. (2013)., A machinability study of mild steel using abrasive water jet machining technology., *Int. J. Eng. Res. Appl*, *3*(3), 1063-1066.

Thangaraj, M., Ahmadein, M., Alsaleh, N. A., & Elsheikh, A. H., Optimization of abrasive water jet machining of SiC reinforced aluminum alloy-based metal matrix composites using Taguchi–DEAR technique, *Materials*, *14*(21), 6250, 2021*anagement*, 2023.

Tolouei-Rad, Majid, Ana Vafadar, and Muhammad Aamir., Impacts of traverse speed and material thickness in abrasive waterjet contour cutting of Austenitic stainless steel AISI 304L, *Applied Sciences*, 11, 4925, 2021.

Tripathi, D. R., Vachhani, K. H., Kumari, S., & Abhishek, K., Experimental investigation on material removal rate during abrasive water jet machining of GFRP composites, *Materials Today: Proceedings*, *26*, 1389-1392, 2020.

Uthayakumar, M. and Rajadurai, A., Surface integrity in AWJM of Inconel 718, *Journal of Mechanical Science and Technology Conference*, pp. 241–248, 2015.

Wen, et al., MACONT: Mixed Aggregation by Comprehensive Normalization Technique for Multi-Criteria Analysis, *INFORMATICA*, Vol. 31, No. 4, 857–880, 2020.

Biographies

Ajit Gaonkar is a research scholar in the Mechanical Engineering Department of Goa College of Engineering (Affiliated to Goa University), Goa, India. He has earned a Bachelor of Engineering degree in Mechanical Engineering and a Master of Engineering in Industrial Engineering from Goa University, India. His research interests include sustainable manufacturing, modelling, simulation & experimental analysis.

Prof. Rajesh S. Prabhu Gaonkar is presently a Professor in Mechanical Engineering at Goa College of Engineering (Affiliated to Goa University), Goa, India. He obtained his doctorate in the field of Reliability Engineering from the Indian Institute of Technology Bombay, India. He was a postdoctoral fellow at the National University of Singapore

(NUS). He has more than 100 research publications that include books, book chapters, journal and conference papers. He has 05 patents to his credit. His research interests include the application of evolving uncertainty theories in Reliability, Maintenance Engineering, and Multi-Attribute Decision Making problems.